

See discussions, stats, and author profiles for this publication at: <https://www.researchgate.net/publication/6418101>

Hydroxide Ion Hydration in Aqueous Solutions

ARTICLE *in* THE JOURNAL OF PHYSICAL CHEMISTRY A · MAY 2007

Impact Factor: 2.69 · DOI: 10.1021/jp0659397 · Source: PubMed

CITATIONS

39

READS

145

2 AUTHORS:



Maciej Smiechowski

Gdansk University of Technology

25 PUBLICATIONS 287 CITATIONS

SEE PROFILE



Janusz Stangret

Gdansk University of Technology

37 PUBLICATIONS 610 CITATIONS

SEE PROFILE

Hydroxide Ion Hydration in Aqueous Solutions

Maciej Śmiechowski and Janusz Stangret*

Department of Physical Chemistry, Chemical Faculty, Gdańsk University of Technology, Narutowicza 11/12, 80-952 Gdańsk, Poland

Received: September 12, 2006; In Final Form: December 1, 2006

Hydroxide ion hydration was studied in aqueous solutions of selected alkali metal hydroxides by means of Fourier transform infrared (FTIR) spectroscopy of HDO isotopically diluted in H₂O. The quantitative difference spectra procedure was applied for the first time to investigate such systems. It allowed removal of bulk water contribution and separation of the spectra of solute-affected HDO. The obtained spectral data were confronted with *ab initio* calculated structures of small gas-phase and polarizable continuum solvation model (PCM) solvated aqueous clusters, OH[−](H₂O)_{*n*}, *n* = 1–7, to establish the structural and energetic states of hydration spheres of the hydrated hydroxide anion. This was achieved by comparison of the calculated optimal geometries with the interatomic distances derived from HDO band positions. The energetic state of water in OH[−] hydration shells, as revealed by solute-affected HDO spectra, is similar to that of an isoelectronic F[−] anion. No evidence was found for the existence of stable hydroxide dimer, H₃O₂[−], in an aqueous solution. Spectral data do confirm, however, existence of a weak interaction with a single water molecule at the hydrogen site of OH[−].

Introduction

The hydroxide anion is a product of autodissociation of water and as such shares with the proton the status of fundamental ions in an aqueous environment. Its importance in acid–base chemistry and in proton-transfer processes encourages detailed studies of its hydration spheres.

The hydroxide anion mobility is anomalously high and is similar to, but still lower than, proton mobility. The observed similarities strongly suggest a congenial microscopic mobility mechanism. Some theoretical considerations have led to solvation and mobility picture essentially resembling the case of hydrated proton, with modifications to the actual transition state in the proton-transfer process.¹

The structure of hydroxide ion aqueous clusters has been the target of computational studies by quantum mechanical (QM) methods.^{2–6} The dynamic picture of solvation mechanism has been provided by molecular dynamics (MD) simulations.^{6–9}

The geometry optimizations of clusters have been recently carried out at the MP2 correlated level with large polarized basis sets.^{2,3} Density functional theory (DFT) approach has also been successfully applied to such systems.^{5,6} The central proton in the simplest hydroxide hydrate, H₃O₂[−], is positioned asymmetrically with respect to two oxygen atoms.^{2,3,6} The calculated oxygen–oxygen distance varies from 2.47 to 2.58 Å.^{2,3,6} There has been some theoretical evidence, however, for existence of a transition state for proton transfer in H₃O₂[−], with oxygen–oxygen distance contracted to ca. 2.4 Å.^{1,4} Higher hydroxide hydrates, OH[−](H₂O)_{*n*}, *n* = 3–5, have been usually found in two isomeric forms: the *C_n* symmetry structure and the OH[−](H₂O)_{*n*−1}(H₂O) structure, with a single water molecule occupying the second hydration shell.^{2–5} Although both forms are true energetic minima, their relative stability has been an ambiguous problem: some authors have identified *C_n* structures as more stable,³ while others have claimed the same about the structures without axial symmetry.⁵

It has been commonly recognized that hydroxide anion is an extremely weak proton donor in hydrogen bond.¹ Computational attempts to obtain stable aqueous clusters with OH[−] donating its hydrogen to a hydrogen bond have usually failed.⁴ A successful convergence of such a structure to an energetic minimum has been reported for a large cluster with no less than 17 solvating water molecules.⁵

Self-consistent reaction field (SCRF) methods, such as the polarizable continuum solvation model (PCM),¹⁰ have provided valuable insights in the studies of external solvent influence on the geometry and energetics of *ab initio* optimized clusters. A coherent method has been recently reported by Pliego and Riveros in the form of cluster-continuum hydration model.¹¹ A similar approach has been formerly applied to hydrated hydroxide ion.⁴ The results obtained, however, have not contradicted previous gas-phase calculations.

Molecular dynamics techniques have provided valuable information about the solvation dynamics and coordination of hydroxide anion in water. In the *ab initio* MD study by Tuckerman et al.,⁹ equilibrium between the dominant planar H₉O₅[−] complex and tetrahedral H₇O₄[−] complex has been detected. The oxygen–oxygen distance from OH[−] to first hydration sphere has been 2.7 Å in the former and 2.6 Å in the latter case. The appearance of more open, tetrahedral structure has been conclusively linked with proton hop occurrence between the anion and a neighboring water molecule. “Hypercoordination” of OH[−] in OH[−](H₂O)₄ has been later confirmed in *ab initio* MD simulations using various DFT functionals.⁸ More recent *ab initio* MD investigation has concluded, on the other hand, that rapid interconversion between tri- and tetra-coordinated OH[−] takes place during the simulation, with OH[−](H₂O)₃ as the dominant structure and rather tight distance to coordinating oxygens (<2.5 Å).⁷

The coordination of OH[−] in an aqueous solution has been briefly studied with X-ray diffraction, and the hydration number of 6 has been found.¹² Recently, very detailed neutron diffraction data, utilizing hydrogen isotope substitution, have been

* To whom correspondence should be addressed. E-mail: stangret@chem.pg.gda.pl.

published.^{13–15} The results are compatible with the H_9O_5^- hydration complex and the presence of a single water molecule weakly coordinated to the hydrogen site of the OH^- ion has been verified.^{14,15} Average hydration number of 5.5 has been also found in dielectric relaxation measurements, although without structural characterization.¹⁶

Vibrational spectroscopy is an ideally suited method for the investigation of solute hydration.^{17,18} Contrary to ample material published for aqueous acidic solutions (see ref 19 for a concise review), aqueous hydroxide solutions have not received such careful attention. Nevertheless, both Raman^{20,21} and IR^{22–25} data are available. An interesting feature of Raman spectra of alkali metal hydroxides in aqueous solution and in crystalline state is the “free OH^- ” band at ca. 3610 cm^{-1} .^{1,20,21,23} It is rather weak in the corresponding IR spectra.²³ Its appearance with only a little red-shift from the gas-phase frequency clearly indicates an at most very weakly hydrogen-bonded H atom, attributable to the OH^- ion.¹ In parallel to the conclusions from hydrated proton spectra, the concept of “very polarizable” hydrogen bonds has been proposed to explain the so-called infrared continua in the vibrational spectra of concentrated solutions of bases.^{22,23} Experimental results from argon predissociation spectroscopy have indicated that the shared proton in gas-phase $\text{OH}^-(\text{H}_2\text{O})$ complex gives rise to an excitation band at 1090 cm^{-1} , connected with delocalization of this proton because of zero-point vibrational motion.²⁶

Spectra of HDO isotopically diluted in H_2O are mostly free from experimental and interpretative problems connected with H_2O spectra.^{27–29} The effects of oscillator coupling dominate the liquid H_2O spectra, especially when strong and polarizable hydrogen bonds are present in the system. On the contrary, the vibrations of decoupled OD oscillators of the HDO molecules function as a very sensitive and ideally suited probe of hydration phenomena, giving valuable structural and energetic information pertaining hydration spheres.

To extract information about the interactions inside the hydration sphere, the contribution of bulk water should be eliminated from the solution spectrum to obtain the solute-affected water spectrum. The relevant method of spectral data analysis was first proposed by Kristiansson et al.^{30,31} The quantitative version of this method was formulated later by these authors and independently in our laboratory.^{32,33} Until now, many ionic solutes have been studied this way and a review summarizing available experimental data has been published.³⁴

The most important factor in the interpretation of HDO spectra is the OD band position. The empirical Badger–Bauer rule states that the position of the water-stretching band changes proportionally to the energy of a hydrogen bond.³⁵ This rule has been extensively tested experimentally,³⁶ also for the water molecule.³⁷ The solute-affected HDO spectra thus give valuable information about the intermolecular energy of perturbed water. In particular, the discrimination between ionic “structure makers” and “structure breakers” (with respect to the bulk phase) is made possible. Further hydration spheres can also be quantitatively characterized.^{34,38} HDO spectra can also provide basic structural characteristics of the solute-affected water, as the OD band position can be correlated with interatomic oxygen–oxygen distance. Several correlations linking R_{OO} with ν_{OD} have been published³⁹ and applied in the studies on ion hydration.^{30,38,40}

Despite its widespread use, the isotopic dilution technique has never before been used in the investigation of hydroxide ion hydration. In this work, we correlate the picture of hydrated hydroxide ion obtained through Fourier transform infrared

(FTIR) measurements of OD band of isotopically diluted HDO molecules with the ab initio calculated structures of small aqueous clusters, $\text{OH}^-(\text{H}_2\text{O})_n$, trying to establish the structural and energetic states of hydration spheres of the hydrated hydroxide ion. The comparison of the calculated optimal geometries with the interatomic distances derived from the HDO band position using the above-mentioned correlation is utilized. The analytically calculated decoupled OD frequencies poorly correlate with experimental results, even when corrected for anharmonicity, and we instead opted for the indirect comparison.

Experimental Section

Chemicals and Solutions. The following crystalline hydroxides were obtained from respectable manufacturers and were used as supplied: $\text{LiOH}\cdot\text{H}_2\text{O}$ (99.95%, Aldrich), NaOH (pure p.a., Chempur), and KOH (pure p.a., Chempur). D_2O used in the preparation of solutions came from two sources: Institute of Nuclear Investigation, Poland (99.84% isotopic purity) and Aldrich (99.96% isotopic purity).

Stock solutions were prepared by mixing weighed amounts of respective solid hydroxides with redistilled water. The molalities of stock solutions were checked by conductometric titration with a standard acid and were $0.984\text{ mol}\cdot\text{kg}^{-1}$ for LiOH, $0.996\text{ mol}\cdot\text{kg}^{-1}$ for NaOH, and $1.032\text{ mol}\cdot\text{kg}^{-1}$ for KOH. The series of solutions, spanning the molality range from ca. $0.2\text{ mol}\cdot\text{kg}^{-1}$ to stock concentration, were prepared by mixing weighed amounts of the respective stock solution with redistilled water. Sample solutions were made by adding 4% (by weight) of D_2O relative to H_2O , and reference solutions were made by adding the same molar amounts of H_2O . Densities of the solutions were interpolated from available highly accurate data.⁴¹

FTIR Measurements and Data Analysis. FTIR spectra were recorded on an IFS 66 Bruker spectrometer. Two hundred and fifty-six scans were made with a selected resolution of 4 cm^{-1} . A cell with CaF_2 windows was employed. The path length was 0.0298 mm , as determined interferometrically. The temperature was kept at $25.0 \pm 0.1\text{ }^\circ\text{C}$ by circulating thermostated water through mounting plates of the cell. The temperature was monitored by a thermocouple inside the cell.

The spectra were handled and analyzed by the commercial PC programs GRAMS/32 (Galactic Industries Corporation, Salem, MA) and RAZOR (Spectrum Square Associates, Ithaca, NY) run under GRAMS/32.

The measured HDO spectra were transformed to molar absorptivity scale and were interpolated from their dependence on molality. The derivative in the infinite dilution approximation, $(\partial\epsilon/\partial m)_{m=0}$, used in our method of spectral data analysis, was then calculated.

The experimental spectra were described equally good by linear or quadratic relationship of molar absorptivity on molality, judging by the determination coefficient value ($R^2 > 0.999$). Generally, nonlinear approximation is the effect of concentration-dependent phenomena, as association, hydrolysis, and so forth. LiOH is thought to be moderately associated and NaOH very slightly associated in aqueous solution^{42,43} (although NaOH was also termed “dissociated electrolyte” on the basis of precise conductivity measurements).⁴³ Assuming a quadratic relationship of ϵ versus m for LiOH gives a very similar shape of solute-affected HDO spectrum and positions of component bands (within experimental error) but higher N value (by about 2) for infinite dilution limit. However, the most consistent and unambiguous results were obtained assuming linear relationships for all three studied hydroxide solutions, and these results are presented and discussed below.

The difference spectra method was used to analyze the influence of solute on the solvent structure. It is based on the assumption that water in the solution may be divided into additive contributions of solute-affected (*a*) and bulk (*b*) water. The “solute-affected” HDO spectra, ϵ_a , were calculated from the derivative spectrum and the bulk HDO spectrum, ϵ_b , according to eq 1.

$$\epsilon_a = \frac{1}{NM} \left(\frac{\partial \epsilon}{\partial m} \right)_{m=0} + \epsilon_b \quad (1)$$

In eq 1, *M* is the mean molecular mass of the solvent (H₂O + 4% D₂O) and *N* is the assumed “affected number”, which means number of moles of solvent affected by one mole of solute.⁴⁰ In the former reports from this laboratory, *N* was also termed “hydration number”.³³ However, *N* is close to hydration number derived from direct methods (e.g., diffraction studies), only when the solute-affected HDO band differs sufficiently from the bulk HDO band, either in position or in half-width. Otherwise, affected number is usually lower than the hydration number. This is particularly true when solute-affected HDO band shape is similar to the bulk HDO band shape. Even then, however, the solute-affected spectrum carries structural-energetic information about greater number of solvent molecules surrounding the solute molecule in reality. This is the main cause of high sensitivity of the method to differentiate various states of solvent molecules in the solution.

The procedure of finding the proper value of *N* by systematic analysis and band-fitting of solute-affected spectra has been previously described in detail.⁴⁰ In brief, the trial solute-affected HDO spectra for trial *N* values are fitted with a sum of linear baseline, analytical bands, and the bulk HDO spectrum. Generally, the minimal number of analytical bands, which gives an adequate fit, is considered as the right number of component bands. Mixed Gaussian–Lorentzian product shape is assumed for all bands at first. All parameters (including Gaussian to Lorentzian ratio) are unconstrained during fit, with the exception of bulk HDO spectrum, for which only intensity is allowed to vary. Bands, for which either Gaussian or Lorentzian contribution is found negligible after convergence, are changed to pure analytical functions, and the fit is repeated. The maximum value of *N* for which the data do not contain a significant contribution of the bulk HDO spectrum is regarded as the affected number and the corresponding ϵ_a spectrum as the final solute-affected spectrum. Usually, the threshold bulk HDO spectrum intensity was taken as 0.5% of the total integrated intensity of the ϵ_a spectrum.

Computational Details

Small aqueous clusters, OH[−](H₂O)_{*n*}, *n* = 1–7, were used as model systems in the calculations. Ab initio calculations were performed with the use of standard Pople basis set 6-311++G(d,p).⁴⁴ In a parallel study of hydrated proton clusters,¹⁹ we found it essentially equivalent to a much more computationally demanding correlation consistent aug-cc-pVTZ basis set, with respect to optimized cluster geometries. Employed basis set is of the triple- ζ type, that is, with triple split valence orbitals, and is augmented with polarization and diffuse functions on both heavy atoms and hydrogens.

Post-HF treatment of electron correlation effects was done in the framework of second-order Møller-Plesset perturbation theory,⁴⁵ with the frozen-core approximation for oxygen inner-core (1s) electrons.

Density functional theory calculations used the B3LYP combination functional,⁴⁶ composed of B88 exchange func-

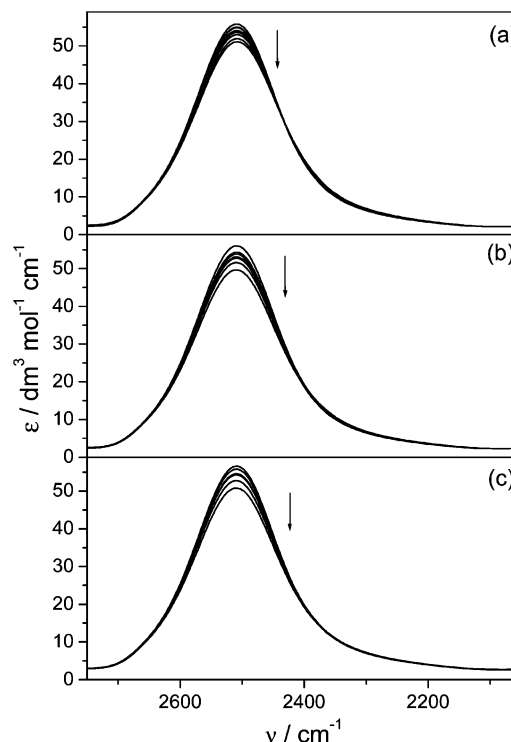


Figure 1. Experimental FTIR spectra of HDO in aqueous solutions of (a) LiOH, (b) NaOH, and (c) KOH in the OD stretching range (arrows indicate molality increase) at 25 °C.

tional⁴⁷ and LYP correlation functional⁴⁸ and containing a portion of Hartree–Fock exchange. Numerical integrations used an *UltraFine* grid, which is a pruned (99 590) grid, consisting of 99 shells per atom and 590 points per shell.

Initial structures of all studied systems belonged to the *C*₁ symmetry group, and no symmetry constraints were imposed during geometry optimizations in the gas-phase. Berny algorithm⁴⁹ with *Tight* convergence criteria was used for optimizations. The GDIIS method⁵⁰ was used for most of the systems to speed up convergence. Vibrational analysis was performed on optimized structures to check for true minima and to calculate zero-point energy (ZPE) corrections.

Gas-phase cluster structures were subsequently used as starting points for further geometry optimization in the SCRF approach. The standard polarizable continuum solvation model (PCM) was used,¹⁰ with united atom topological model applied on atomic radii of the UFF force field (UA0), as implemented in the Gaussian 03 system.⁵¹ Vibrational analysis for PCM optimized structures was performed in the numeric approximation.

All calculations were performed with the Gaussian 03 system.⁵¹ HyperChem 6.0 (Hypercube, Inc., Gainesville, FL) and GaussView 3.0 (Gaussian, Inc., Pittsburgh, PA) served as front-end interfaces and visualization tools.

Results and Discussion

Solute-Affected HDO Spectra. The measured HDO spectra in the ν_{OD} band region for the three studied bases are shown in Figure 1 and the corresponding derivatives $(\partial \epsilon / \partial m)_{m=0}$ are shown in Figure 2. The solute-affected HDO spectra, calculated from eq 1, are shown in Figure 3. The following affected numbers were found after the adjustment procedure: *N* = 6.9 (LiOH), *N* = 9.1 (NaOH), and *N* = 8.8 (KOH). The estimated maximal error in *N* value is ± 1.0 .⁴⁰ The *N* values observed here compare favorably with our results for alkali metal hexafluorophosphates,

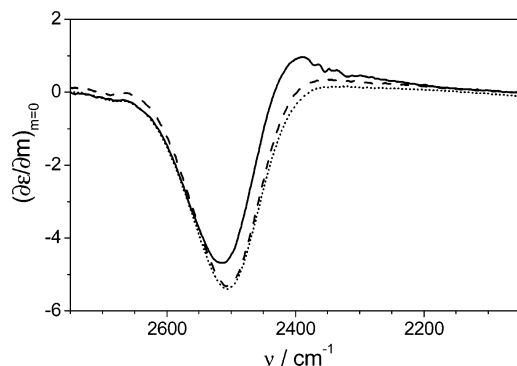


Figure 2. Derivatives $(\partial\epsilon/\partial m)_{m=0}$ in the OD stretching region for aqueous solutions of LiOH (solid line), NaOH (dashed line), and KOH (dotted line) for linear relationship of ϵ vs m .

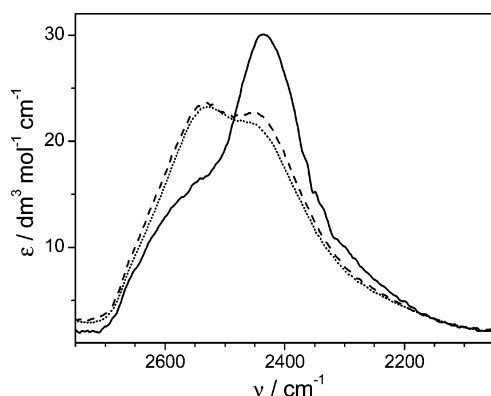


Figure 3. Solute-affected HDO spectra in the OD stretching region for LiOH (solid line), NaOH (dashed line), and KOH (dotted line) aqueous solutions.

where we have found $N = 6.6$ for LiPF_6 , $N = 7.7$ for NaPF_6 , and $N = 9.8$ for KPF_6 .³⁸ The spectra of HDO affected by alkali metal hydroxides were not fundamentally different from other electrolytes studied in our group.^{33,34,38,40} More importantly, they were quite dissimilar to the results obtained lately by us for the hydrated proton.¹⁹ Unlike for the infrared spectra of solutions of strong bases in H_2O , the structure of the solute-affected HDO spectra cannot be adequately described as a “continuum”.^{22,23} Instead, they could be precisely resolved into simple component bands.

The decomposition of the solute-affected HDO spectra into components is depicted in Figure 4, and the respective most important parameters are listed in Table 1. Tentatively, the most pronounced band at ca. 2440 cm^{-1} is assigned to the anion-affected HDO and the second largest band at ca. 2548 cm^{-1} is assigned to the cation-affected HDO, on the basis of available data.³⁴ The alkali metal cation-affected HDO was previously studied by us in considerable detail,³⁸ and independent results from other laboratories have been also reviewed.³⁴ The position of cation-affected water band was 2543 cm^{-1} , but the Li^+ -affected HDO band contained another component at 2445 cm^{-1} (for other cations it manifested only as a slight asymmetry of the main band). In the present work, this band was slightly blue-shifted to $2550\text{--}2546\text{ cm}^{-1}$ (Table 1). The previously observed weak low-wavenumber component was obscured by the much more intensive band attributed to the hydrated hydroxide ion.

To extract more specific information about the hydration spheres of OH^- from the solute-affected HDO spectra, we eliminated the cationic contribution from the spectra by subtracting the reference spectrum of a respective cation. The reference spectra were obtained previously for alkali metal hexafluorophosphates.³⁸ The PF_6^- anion is unique in its

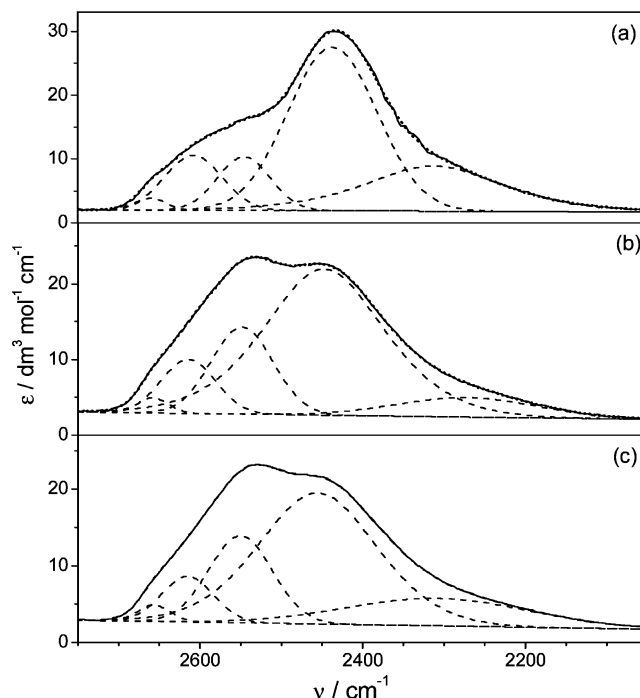


Figure 4. Decomposition of the solute-affected HDO spectra into component bands for (a) LiOH, (b) NaOH, and (c) KOH. Solid line: original spectrum, dashed lines: component bands, dotted line: sum of the component bands.

TABLE 1: Parameters of Component Bands from the Decomposition of the Spectra of HDO Affected by LiOH, NaOH, and KOH

LiOH			NaOH			KOH		
$\nu_{\text{OD}}^{\text{a}}$	fwhh ^b	I ^c	$\nu_{\text{OD}}^{\text{a}}$	fwhh ^b	I ^c	$\nu_{\text{OD}}^{\text{a}}$	fwhh ^b	I ^c
2660	43	83	2658	46	94	2656	49	106
2608	85	764	2613	79	596	2615	78	472
2546	78	682	2548	92	1094	2550	92	1111
2438	129	3503	2448	174	3697	2455	173	3172
2313	194	1473	2272	199	519	2309	258	903

^a Band position at maximum (cm^{-1}). ^b Full width at half-height (cm^{-1}). ^c Integrated intensity ($\text{dm}^3\cdot\text{mol}^{-1}\cdot\text{cm}^{-1}$).

structure-breaking properties in water, and a perfect separation of anion- and cation-affected HDO could be achieved. The PF_6^- anion-affected component band was then subtracted from the solute-affected HDO band to reveal the purely cationic influence. This approach is still somewhat arbitrary, as the influence of cation and anion on the spectrum of HDO is certainly cooperative.³⁸ Nevertheless, the internal consistence of the hydroxide anion-affected HDO spectra derived from three independent electrolyte series in this work proves that good quality “single-ion” HDO spectra can be derived and subsequently used, when the separation of anion- and cation-affected bands is sufficient, as was certainly the case of alkali metal cations and PF_6^- anion.³⁸ Equation 2 was used to calculate the hydroxide ion-affected spectra from the solute-affected HDO spectra, ϵ_{MOH} , and the reference cation spectra, ϵ_{M} .

$$\epsilon_{\text{OH}} = \epsilon_{\text{MOH}} - \alpha \epsilon_{\text{M}} \quad (\text{M} = \text{Li, Na, K}) \quad (2)$$

The subtraction factor α was determined by systematic analysis, similar to the procedure of finding the solute-affected solvent spectrum in the difference spectra method.⁴⁰ The proper value of α was found on the basis of fitting the trial ϵ_{OH} spectrum with analytical bands and the reference cation spectrum ϵ_{M} . The smallest possible value of α , for which the contribution

TABLE 2: Parameters of Component Bands from the Decomposition of the Spectra of HDO Affected by Hydroxide Anion in LiOH, NaOH, and KOH Aqueous Solutions

LiOH			NaOH			KOH		
$\nu_{\text{OD}}^{\text{a}}$	fwhh ^b	I ^c	$\nu_{\text{OD}}^{\text{a}}$	fwhh ^b	I ^c	$\nu_{\text{OD}}^{\text{a}}$	fwhh ^b	I ^c
2658	33	97	2658	37	127	2658	36	152
2604	94	1012	2604	93	983	2600	96	962
2432	115	5343	2438	141	6682	2440	151	6268
2340	227	4398	2338	265	3664	2318	270	3001

^a Band position at maximum (cm^{-1}). ^b Full width at half-height (cm^{-1}). ^c Integrated intensity ($\text{dm}^3 \cdot \text{mol}^{-1} \cdot \text{cm}^{-1}$), scaled per one mole of hydroxide-affected HDO.

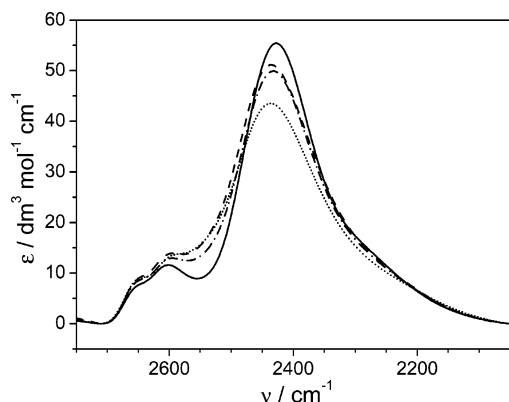


Figure 5. OH^- -affected HDO spectra (ϵ_{OH}) in the OD stretching region, obtained from LiOH (solid line), NaOH (dashed line), and KOH (dotted line) affected HDO spectra, scaled per one mole of hydroxide-affected water, and the average ϵ_{OH} spectrum (dashed–dotted line).

of ϵ_{M} was still insignificant, was regarded as the final adjusted value of this parameter, and the corresponding ϵ_{OH} spectrum was treated as the final refined hydroxide ion-affected HDO spectrum.

The finally obtained α values were equal to 0.196 for LiOH, 0.4 for NaOH, and 0.385 for KOH. The parameters of the analytical bands for respective fits of ϵ_{OH} are listed in Table 2. It can be readily observed that eliminating the cationic influence (and the band at 2548 cm^{-1}) resulted in much more coherent values than those presented in Table 1. The spectra, scaled per one mole of hydroxide-affected HDO, are presented in Figure 5. The average of the three ϵ_{OH} spectra obtained for three different hydroxides was almost equal to the ϵ_{OH} spectrum derived from ϵ_{NaOH} .

The first noteworthy feature of the OH^- -affected HDO spectrum was the presence of a weak, yet clearly visible band at 2658 cm^{-1} , unusually blue-shifted when compared to other electrolytes.³⁴ The above-mentioned “free OH^- ” band has been observed in the Raman spectra of hydroxide aqueous solutions at ca. 3610 cm^{-1} .^{1,20,21,23} This feature has rarely been detected in the infrared as a very weak band,²³ apparently because of high symmetry of the corresponding normal mode, making it only Raman active.¹ The frequency of this band in infrared spectrum of H_2O could be directly converted to the OD stretching band position of HDO by means of an available ν_{OH} versus ν_{OD} correlation on the basis of spectroscopic data for solid hydrates.⁵² The ν_{OH} value of 3610 cm^{-1} corresponds to the ν_{OD} value of 2658 cm^{-1} ; the agreement with the HDO spectra presented here is remarkable. Thus, the most blue-shifted component band in the OH^- -affected spectra may be unambiguously ascribed to isotopically substituted OD^- ions present in aqueous solution. Its appearance in the hydroxide-affected HDO

spectra most probably results from isotopic decoupling and symmetry perturbation.

The outermost hydration sphere of the cation, influenced by the anion and detectable with our method of analysis, manifests itself by a single band in the solute-affected HDO spectra.³⁸ For alkali metal cations studied in this work, the discussed band represented the second hydration sphere. The position of this band depended approximately linearly on the band position of affected HDO for the counteranion. The value found in the present work is 2603 cm^{-1} , in good agreement with the published correlation.³⁸ One might suspect that this band should disappear upon subtraction of cation-affected spectrum, but the reference spectra were recorded for different electrolytes (with PF_6^- as counteranion), where a similar band was significantly blue-shifted to 2631 cm^{-1} .³⁸

The main band of the OH^- -affected HDO spectrum was located at 2437 cm^{-1} on average. This spectral component displayed also a red-shifted tail centered on average at 2332 cm^{-1} . Taken together, these two analytical bands appear as a single asymmetric curve (viz., the overall band shape in Figure 5). Though in principle it is possible to approximate this shape with a single analytical curve (say, log-normal),³³ we found previously that inclusion of a separate component to describe the tail of the main band provided a much better fit.³⁸ The shape and position of the OH^- -affected HDO band is very similar to the case of fluoride anion, previously studied in our laboratory,⁴⁰ for which the F^- -affected HDO band was located at 2433 cm^{-1} and displayed similar pronounced tail at lower wavenumbers. Thus, hydroxide anion appears to be one of the very few structure-making anions in aqueous solution.³⁴

The ascription of the component bands to certain energetic situations of water molecules in the hydration spheres may be achieved by transforming HDO band position, ν_{OD} , to intermolecular interaction energy of water, ΔU_{w} . The relationship linking ΔU_{w} with ν_{OD} takes advantage of the Badger–Bauer rule,³⁵ and the numerical procedure for HDO has been described before.³⁴ The calculated value of ΔU_{w} for ν_{OD} obtained for the hydroxide anion in this work (2437 cm^{-1}) is $-56.2 \text{ kJ mol}^{-1}$. The experimental absolute enthalpy of hydration of OH^- is -529 kJ mol^{-1} .⁵³ These two values combined neatly fit into the available correlation line for halide anions and they situate OH^- very near to F^- on that line.³⁴

Further interpretation of the OH^- -affected spectra, in view of the interatomic oxygen–oxygen distances, calculated from the band positions, is presented below in comparison with the ab initio obtained cluster geometries.

Ab Initio Results. Figure 6 shows the structures studied in this work in their optimized gas-phase geometries. The only geometric parameter suitable for comparison with the HDO spectra is the interatomic oxygen–oxygen distance, R_{OO} . The calculated gas-phase R_{OO} values are shown in Table 3. The geometry of the studied clusters was fairly conserved between various methods, although an elongation of interatomic distances in B3LYP versus MP2 level of theory might be generally observed. The difference in R_{OO} , however, did not exceed 0.044 \AA in the extreme case of $\text{OH}^-(\text{H}_2\text{O})_3$. The geometries obtained by us for the smallest clusters, $n = 1-3$, were in good agreement with the MP2/aug-cc-pVDZ structures published by Xantheas.² Our results were also comparable to DFT calculations by Wei et al. using 6-311++G** basis set and BLAP3 and B3LYP functionals.⁶ Larger clusters, $n = 4$, were similar to those obtained by Novoa et al. at BLYP/6-31+G(2d,2p) level,⁵ although their oxygen–oxygen distances were somewhat shorter. Also, the single second-sphere water molecule was always in a

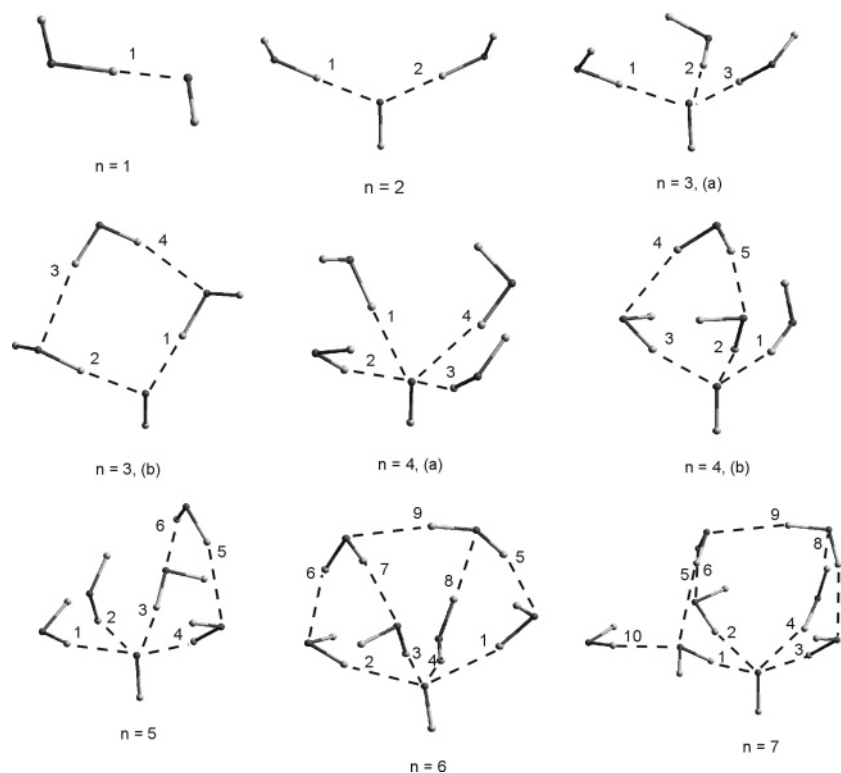


Figure 6. Hydrated hydroxide anion clusters, $\text{OH}^-(\text{H}_2\text{O})_n$, studied in this work, in their B3LYP/6-311++G(d,p) gas-phase optimized geometries. Red spheres denote oxygens, gray spheres denote hydrogens. The numbers over hydrogen bonds refer to columns in Tables 3 and 4.

TABLE 3: Optimized Intermolecular Oxygen–Oxygen Distances, R_{OO} , in the Studied $\text{OH}^-(\text{H}_2\text{O})_n$ Gas-Phase Clusters

n	level of theory	R_{OO}^a									
		1	2	3	4	5	6	7	8	9	10
1	DFT ^b	2.479									
	MP2 ^c	2.474									
2	DFT	2.575	2.575								
	MP2	2.568	2.561								
3 ^d	DFT	2.637	2.637	2.637							
	(a) MP2	2.681	2.606	2.595							
3 ^e	DFT	2.531	2.558	2.944	2.904						
	(b) MP2	2.522	2.540	2.943	2.920						
4 ^d	DFT	2.716	2.716	2.716	2.716						
	(a) MP2	2.700	2.700	2.700	2.700						
4 ^e	DFT	2.743	2.557	2.616	2.958	2.892					
	(b) MP2	2.724	2.538	2.603	2.961	2.887					
5	DFT	2.857	2.797	2.574	2.695	2.932	2.912				
	MP2	2.892	2.780	2.548	2.658	2.937	2.912				
6	DFT	2.708	2.736	2.591	2.872	2.890	2.868	2.902	2.928	2.917	
	MP2	2.693	2.698	2.574	2.873	2.869	2.864	2.895	2.943	2.915	
7	DFT	2.584	2.705	2.650	2.944	2.933	2.884	2.881	2.913	2.906	2.964
	MP2	2.565	2.659	2.645	2.924	2.936	2.864	2.867	2.925	2.905	2.957

^a All distances in Å, the numbers refer to respective labels in Figure 4. ^b B3LYP/6-311++G(d,p) optimization. ^c MP2/6-311++G(d,p) optimization. ^d $\text{OH}^-(\text{H}_2\text{O})_n$ structure. ^e $\text{OH}^-(\text{H}_2\text{O})_{n-1}(\text{H}_2\text{O})$ structure.

“bridging” position (Figure 6), much like in the most stable isomers found in Novoa et al.’s paper.⁵ Independently of the cluster size, tetracoordinated structure was preferred around the ion’s oxygen atom for larger clusters ($n > 4$). The relative stability of the studied systems differed only slightly with respect to computational method (see Supporting Information section for details of cluster energies). The trihydrated hydroxide anion was more stable in the pseudo- C_3 form than in the $\text{OH}^-(\text{H}_2\text{O})_2(\text{H}_2\text{O})$ isomer by ca. 10 kJ mol^{−1} (including scaled zero-point correction). On the other hand, no immediate preference could be deduced for either isomer of $\text{OH}^-(\text{H}_2\text{O})_4$ cluster; the difference in electronic (+zero-point) energy was at most about thermal energy term (RT) at 298 K.

Including external solvent field via PCM approach did not result in significant changes of most interatomic distances (Table 4). A prominent difference was noted only for $\text{OH}^-(\text{H}_2\text{O})$ structure, where the length of the single hydrogen bond increased by ca. 0.06 Å, approaching the respective distances in larger clusters. This suggests that contrary to the hydrated proton case, very short hydrogen bonds (<2.5 Å) should not be expected around hydroxide anion in an aqueous solution. On the other hand, a slight contraction of bonds in the first and the second hydration spheres in larger clusters could be noticed.

Surprisingly, the axially (pseudo-)symmetric structures failed to converge as energetic minima in the PCM approximation. Either transition structures were obtained or higher-order saddle

TABLE 4: Optimized Intermolecular Oxygen–Oxygen Distances, R_{OO} , in the Studied $\text{OH}^-(\text{H}_2\text{O})_n$ PCM Model Clusters

n	level of theory	R_{OO}^a									
		1	2	3	4	5	6	7	8	9	10
1	DFT ^b	2.541									
	MP2 ^c	2.540									
2	DFT	2.589	2.589								
	MP2	2.580	2.580								
3 ^d	DFT	2.559	2.567	2.820	2.816						
(b)	MP2	2.542	2.552	2.818	2.812						
4 ^d	DFT	2.683	2.594	2.592	2.830	2.841					
(b)	MP2	2.664	2.572	2.570	2.820	2.833					
5	DFT	2.776	2.733	2.640	2.664	2.818	2.812				
	MP2	2.767	2.718	2.612	2.628	2.808	2.804				
6	DFT	2.662	2.668	2.672	2.790	2.811	2.808	2.808	2.963	2.857	
	MP2	2.638	2.647	2.647	2.774	2.793	2.797	2.791	2.981	2.846	
7	DFT	2.639	2.642	2.670	2.801	2.852	2.843	2.806	2.950	2.855	2.851
	MP2	2.617	2.612	2.651	2.789	2.841	2.823	2.790	2.969	2.844	2.844

^a All distances in Å, the numbers refer to respective labels in Figure 4. ^b B3LYP/6-311++G(d,p) optimization. ^c MP2/6-311++G(d,p) optimization. ^d $\text{OH}^-(\text{H}_2\text{O})_{n-1}(\text{H}_2\text{O})$ structure.

TABLE 5: Average Intermolecular Oxygen–Oxygen Distances in Different Structural Positions in the Studied $\text{OH}^-(\text{H}_2\text{O})_n$ Clusters and the Corresponding Vibrational Frequencies

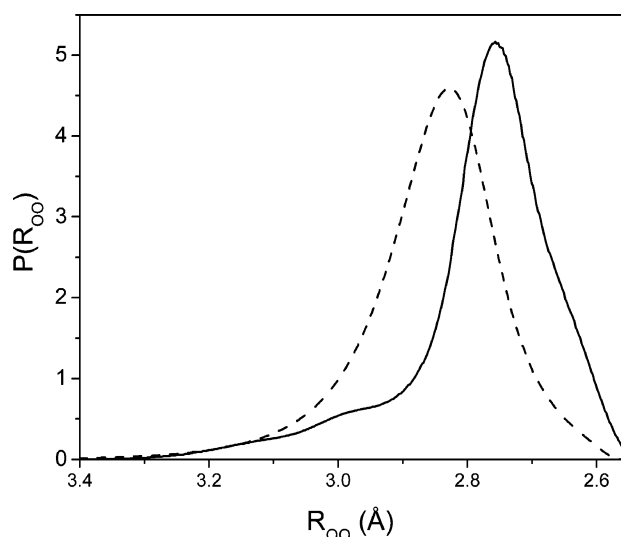
interpretation ^a	level of theory	gas-phase		PCM	
		R_{OO}^b	ν_{OD}^c	R_{OO}^b	ν_{OD}^c
first hydration sphere	B3LYP/6-311++G(d,p)	2.679	2316	2.659	2286
	MP2/6-311++G(d,p)	2.663	2292	2.640	2252
second hydration sphere	B3LYP/6-311++G(d,p)	2.913	2556	2.844	2505
	MP2/6-311++G(d,p)	2.912	2555	2.836	2499

^a See text for classification details. ^b Average oxygen–oxygen distance within the hydration sphere, taken over all clusters (Å). ^c OD stretching band position (cm^{-1}) calculated from the average distance.⁴⁴

points (on the basis of the number of imaginary vibrational frequencies) were obtained. The structure presented by Tunon et al. for $\text{OH}^-(\text{H}_2\text{O})_3$ in a continuum (an “umbrella-like” cluster with free-water hydrogens pointing in the direction marked by OH^- hydrogen)⁴ was a third-order saddle point from our calculations. Certainly, the choice of proper ionic radii for building atomic cavities in the continuous solvent was a crucial issue. From the tested models, only UA0 atomic radii, on the basis of UFF force field,⁵¹ provided stable energetic minima after optimization. Nevertheless, even in this approach the C_n structures proved to be unstable.

Proposed Molecular Model of Hydroxide Anion Hydration. The comparison of experimental and computational results was made possible by comparing HDO vibrational frequencies predicted from optimized structures with those resulting from decomposition of the OH^- -affected spectra into analytical components.

To facilitate the mentioned comparison, ab initio obtained oxygen–oxygen distances were grouped into classes reflecting different structural situations. Water molecules directly hydrogen-bonded to OH^- were collectively termed as “first hydration sphere” and the respective R_{OO} values from all studied clusters formed the first class, with the exception of $\text{OH}^-(\text{H}_2\text{O})$ dimer, omitted as an atypical case. All other hydrogen-bonded distances in the systems were grouped into “second hydration sphere” class. The average R_{OO} values were then calculated for both classes, depending on level of theory, separately for gas-phase and PCM calculations (viz., Table 5). The average distances, thus obtained, were next transformed into average OD band positions. We used the R_{OO} versus ν_{OD} correlation curve of

**Figure 7.** Interatomic oxygen–oxygen distance distribution derived from the average OH^- -affected HDO spectrum (solid line) along with bulk HDO distance distribution curve (dashed line).

Berglund et al.³⁹ Average theoretical ν_{OD} values may be compared with the experimental values from Table 2.

It is readily seen that ab initio derived average ν_{OD} for HDO molecules directly hydrogen-bonded to the anion was red-shifted with respect to experiment by ca. 122–146 cm^{-1} for gas-phase calculations and as much as 152–186 cm^{-1} for PCM calculations, taking the average experimental band position as 2437 cm^{-1} . Even considering the asymmetry of the experimental HDO band, it is a major disagreement. The probable reason is the overestimation of strong hydrogen bonds in ab initio calculations on limited-size clusters. In ab initio MD simulations of $\text{OH}^-(\text{H}_2\text{O})_{31}$, R_{OO} to the first hydration sphere has been close to 2.7 Å,^{8,9} which is still about 0.07 Å lower than the estimate from the OH^- -affected HDO band position. Concentration-dependent effects may also be responsible for the observed band shift and caution should be taken when comparing the present experimental results to computational and diffraction studies, where concentration of the solute is usually much higher.

Apart from the simple band position with distance correlation, our approach has also allowed calculation of distance probability distribution curves from absorption band shapes,^{38,40} as proposed before.³¹ The numerical procedure and assumptions to the method have been discussed in detail.⁴⁰ Figure 7 compares $P(R_{OO})$ versus R_{OO} curves for bulk HDO and for average

OH[−]-affected HDO. Because of the asymmetry of probability distribution curves, two parameters are relevant: the maximum of distribution function, R_{OO}^0 , reflecting the most probable distance, and the position of gravity center, R_{OO}^g , reflecting mean distance.⁴⁰ The average values found for OH[−]-affected HDO from the three hydroxides were $R_{OO}^0 = 2.755 \pm 0.007$ Å and $R_{OO}^g = 2.762 \pm 0.016$ Å, while for bulk HDO they were 2.827 Å and 2.836 Å, respectively.

Even more important is the theoretical result for the second hydration sphere. Although the gas-phase value for average ν_{OD} was 2556 cm^{−1}, in the PCM approximation it was red-shifted to ca. 2500 cm^{−1}, remarkably close to the bulk HDO band position in liquid H₂O, which we found at 2509 cm^{−1}. This implies that well-defined solvation structure of hydroxide anion does not extend further than its first hydration sphere, making it quite different from the hydrated proton¹⁹ but similar to all other anions, which do not show multiple hydration layers in the HDO spectra.³⁴

Solute-affected number obtained by our spectral analysis method for the whole electrolyte can be divided into ionic contributions only with arbitrary assumptions.⁴⁰ If we attempt to divide the N parameter into ionic contributions, it is safe to assume coordination number for metal cation known from other (e.g., diffraction studies) sources.³² Anion hydration number can then be calculated with the help of eq 3.

$$N = N_C + 0.5 N_A \quad (3)$$

N_C and N_A are hydration numbers of cation and anion, respectively, and N is the affected number. The factor 0.5 comes from the fact that HDO molecule can interact with the anion either through its hydrogen or deuterium atom, and only in the latter case it is considered "affected". If isotopic fractionation effects are negligible, there is an equal number of HDO molecules in both situations, hence the 0.5 factor.³²

The typical alkali metal cations, like Na⁺ or K⁺, have been known to be hexacoordinated in water (although coordination numbers derived by diffraction methods may be in error by ± 1).^{54,55} If we take $N = 9$ and $N_C = 6$, we get $N_A = 2(9 - 6) = 6$ for the hydration number of OH[−] in water. This includes all HDO molecules statistically perturbed by the anion, but also the anion itself, since it undergoes isotopic substitution in D₂O-enriched system. That leaves five OH[−]-affected HDO molecules, possibly four molecules in an OH[−](H₂O)₄ complex and a single water molecule located at the hydrogen site of the anion.

Recent diffraction studies indicate OH[−](H₂O)₄ as the prominent complex in an aqueous solution.^{13–15} More importantly, oxygen–oxygen distance to the first hydration sphere computed by us from the OH[−]-affected spectra was closer to MD results quoted for the tetracoordinated anion (2.7 Å) than for the tricoordinated case (2.6 Å).⁹ Since R_{OO} versus ν_{OD} correlation is firmly established for all but the shortest hydrogen bonds,³⁹ this observation is the strongest premise for dominance of OH[−](H₂O)₄ complex that can be deduced from hydroxide-affected HDO spectra.

From these indirect clues, we infer that OH[−](H₂O)₄ is probably the basic structural unit in an aqueous solution. This does not exclude the possibility of equilibrium between tri- and tetracoordinated structures, as predicted by numerous MD simulations.^{7–9} Transient structures accompanying proton transfer, however, were not detected in the OH[−]-affected spectra, since very short hydrogen bonds would manifest themselves by unusually red-shifted component bands in the solute-affected HDO spectrum.¹⁹

Conclusions

Ab initio optimized geometries of small aqueous clusters can aid in the interpretation of solute-affected HDO spectra, particularly for nontrivial solutes. Reoptimization of the clusters in the continuous solvent allowed us to verify experimental data with more certainty and thus seemed necessary for deeper understanding of the structure of aqueous solutions.

Upon subtraction of alkali metal reference spectra obtained previously,³⁸ we were able to determine the OH[−]-affected HDO spectrum with high certainty. The energetic state of water in OH[−] hydration shells, as revealed by OH[−]-affected HDO spectra, is similar to that of an isoelectronic F[−] anion.⁴⁰ A broad component centered on average at 2437 cm^{−1}, with a low-wavenumber tail centered at 2332 cm^{−1}, could be attributed to the hydroxide anion. Mean oxygen–oxygen distance computed from the contour of the OH[−]-affected spectrum was 2.762 Å. Computations predict a shorter hydrogen bond length, but a qualitative agreement with experiment was obtained. Furthermore, second hydration sphere was found to resemble bulk water on average, especially in the PCM calculations. Correspondingly, no features in the OH[−]-affected spectrum could be assigned to this sphere, although it has been a common occurrence for cations.³⁴ Isotopic decoupling allowed us to detect the "free" OD[−] stretching mode at 2658 cm^{−1}, formerly identified in Raman spectra of alkali solutions in H₂O at 3610 cm^{−1}.^{20,21,23} It was unusually blue-shifted for an HDO band, suggesting only a very weak interaction at the hydrogen site of the anion.

No evidence was found for the existence of stable hydroxide dimer, H₃O₂[−], in an aqueous solution. Such strongly hydrogen-bonded structure would manifest itself in the solute-affected spectra by component bands significantly more red-shifted than those found in the present work. This makes hydroxide anion quite different from the hydrated proton, for which discussed features were actually detected.¹⁹

Acknowledgment. Calculations in Gaussian 03 were carried out at the Academic Computer Center in Gdańsk (TASK). Financial support from Center of Excellence in Environmental Analysis & Monitoring in Gdańsk (CEEAM) in the purchase of Gaussian 03W and GaussView 3.0 programs is acknowledged. Experimental work was supported by internal grants from Gdańsk University of Technology.

Supporting Information Available: Energies of the studied OH[−](H₂O)_{*n*} gas-phase clusters (Table S1). This material is available free of charge via the Internet at <http://pubs.acs.org>.

References and Notes

- (1) Agmon, N. *Chem. Phys. Lett.* **2000**, *319*, 247.
- (2) Xantheas, S. *J. Am. Chem. Soc.* **1995**, *117*, 10373.
- (3) Masamura, M. *J. Mol. Struct. (THEOCHEM)* **2000**, *498*, 87.
- (4) Tuñón, I.; Rinaldi, D.; Ruiz-López, M. F.; Rivail, J. L. *J. Phys. Chem.* **1995**, *99*, 3798.
- (5) Novoa, J. J.; Mota, F.; del Valle, C. P.; Planas, M. *J. Phys. Chem. A* **1997**, *101*, 7842.
- (6) Wei, D.; Proynov, E. I.; Milet, A.; Salahub, D. R. *J. Phys. Chem. A* **2000**, *104*, 2384.
- (7) Asthagiri, D.; Pratt, L. R.; Kress, J. D.; Gomez, M. A. *Proc. Natl. Acad. Sci.* **2004**, *101*, 7229.
- (8) Tuckerman, M. E.; Chandra, A.; Marx, D. *Acc. Chem. Res.* **2006**, *39*, 151.
- (9) Tuckerman, M. E.; Laasonen, K.; Sprik, M.; Parrinello, M. *J. Phys. Chem.* **1995**, *99*, 5749.
- (10) Cossi, M.; Barone, V.; Cammi, R.; Tomasi, J. *Chem. Phys. Lett.* **1996**, *255*, 327.
- (11) Pliego, J. R.; Riveros, J. M. *J. Phys. Chem. A* **2001**, *105*, 7241.
- (12) Brady, G. W. *J. Chem. Phys.* **1958**, *28*, 464.

- (13) Bruni, F.; Ricci, M. A.; Soper, A. K. *J. Chem. Phys.* **2001**, *114*, 8056.
- (14) Botti, A.; Bruni, F.; Imberti, S.; Ricci, M. A.; Soper, A. K. *J. Chem. Phys.* **2003**, *119*, 5001.
- (15) Botti, A.; Bruni, F.; Imberti, S.; Ricci, M. A.; Soper, A. K. *J. Chem. Phys.* **2004**, *120*, 10154.
- (16) Buchner, R.; Heftner, G.; May, P. M.; Sipos, P. *J. Phys. Chem. B* **1999**, *103*, 11186.
- (17) Verrall, R. E.; Lilley, T. H.; Conway, B. E.; Luck, W. A. P. In *Water, A Comprehensive Treatise*, Vol. 3; Franks, F., Ed.; Plenum: New York, 1973.
- (18) Conway, B. E. *Ionic Hydration in Chemistry and Biophysics*; Elsevier: Amsterdam, 1981; Chapters 7 and 8.
- (19) Śmiechowski, M.; Stangret, J. *J. Chem. Phys.* **2006**, *125*, 204508.
- (20) Busing, W. R.; Hornig, D. F. *J. Phys. Chem.* **1961**, *65*, 284.
- (21) Buanam-Om, C.; Luck, W. A. P.; Schiöberg, D. *Z. Phys. Chem. (N. F.)* **1979**, *117*, 19.
- (22) Schiöberg, D.; Zundel, G. *J. Chem. Soc., Faraday Trans. 2* **1973**, *69*, 771.
- (23) Librovich, N. B.; Sakun, V. P.; Sokolov, N. D. *Chem. Phys.* **1979**, *39*, 351.
- (24) Ackermann, T. *Z. Phys. Chem. (N. F.)* **1961**, *27*, 253.
- (25) Rhine, P.; Williams, D.; Hale, G. M.; Query, M. R. *J. Phys. Chem.* **1974**, *78*, 1405.
- (26) Diken, E. G.; Headrick, J. M.; Roscioli, J. R.; Bopp, J. C.; Johnson, M. A.; McCoy, A. B.; Huang, X.; Carter, S.; Bowman, J. M. *J. Phys. Chem. A* **2005**, *109*, 571.
- (27) Waldron, R. D. *J. Chem. Phys.* **1957**, *26*, 809.
- (28) Hornig, D. F. *J. Chem. Phys.* **1964**, *40*, 3119.
- (29) Falk, M.; Ford, T. A. *Can. J. Chem.* **1966**, *44*, 1699.
- (30) Kristiansson, O.; Eriksson, A.; Lindgren, J. *Acta Chem. Scand. A* **1984**, *38*, 609.
- (31) Kristiansson, O.; Eriksson, A.; Lindgren, J. *Acta Chem. Scand. A* **1984**, *38*, 613.
- (32) Kristiansson, O.; Lindgren, J.; de Villepin, J. *J. Phys. Chem.* **1988**, *92*, 2680.
- (33) Stangret, J. *Spectrosc. Lett.* **1988**, *21*, 369.
- (34) Stangret, J.; Gampe, T. *J. Phys. Chem. A* **2002**, *106*, 5393 and references therein.
- (35) Badger, R. M.; Bauer, S. H. *J. Chem. Phys.* **1937**, *5*, 839.
- (36) Rao, C. N. R.; Dwivedi, P. C.; Ratajczak, H.; Orville-Thomas, W. *J. J. Chem. Soc., Faraday Trans. 2* **1975**, *71*, 955.
- (37) Bricknell, B. C.; Ford, T. A.; Letcher, T. M. *Spectrochim. Acta, Part A* **1997**, *53*, 299.
- (38) Śmiechowski, M.; Gojlo, E.; Stangret, J. *J. Phys. Chem. B* **2004**, *108*, 15938.
- (39) Berglund, B.; Lindgren, J.; Tegenfeldt, J. *J. Mol. Struct.* **1978**, *43*, 179.
- (40) Stangret, J.; Gampe, T. *J. Phys. Chem. B* **1999**, *103*, 3778.
- (41) Herrington, T. M.; Pethybridge, A. D.; Roffey, M. G. *J. Chem. Eng. Data* **1986**, *31*, 31.
- (42) Burgess, J. *Metal Ions in Solution*; Ellis Horwood, Ltd.: Chichester, U.K., 1978; p 264.
- (43) Corti, H.; Crovetto, R.; Fernández-Prini, R. *J. Solution Chem.* **1979**, *12*, 897.
- (44) Krishnan, R.; Binkley, J. S.; Seeger, R.; Pople, J. A. *J. Chem. Phys.* **1980**, *72*, 650.
- (45) Møller, C.; Plesset, M. S. *Phys. Rev.* **1934**, *46*, 618.
- (46) Becke, A. D. *J. Chem. Phys.* **1993**, *98*, 5648.
- (47) Becke, A. D. *Phys. Rev. A* **1988**, *38*, 3098.
- (48) Lee, C.; Yang, W.; Parr, R. G. *Phys. Rev. B* **1993**, *37*, 785.
- (49) Schlegel, H. B. *J. Comp. Chem.* **1982**, *3*, 214.
- (50) Csaszar, P.; Pulay, P. *J. Mol. Struct. (THEOCHEM)* **1984**, *114*, 31.
- (51) Frisch, M. J.; Trucks, G. W.; Schlegel, H. B.; Scuseria, G. E.; Robb, M. A.; Cheeseman, J. R.; Montgomery, J. A., Jr.; Vreven, T.; Kudin, K. N.; Burant, J. C.; Millam, J. M.; Iyengar, S. S.; Tomasi, J.; Barone, V.; Mennucci, B.; Cossi, M.; Scalmani, G.; Rega, N.; Petersson, G. A.; Nakatsuji, H.; Hada, M.; Ehara, M.; Toyota, K.; Fukuda, R.; Hasegawa, J.; Ishida, M.; Nakajima, T.; Honda, Y.; Kitao, O.; Nakai, H.; Klene, M.; Li, X.; Knox, J. E.; Hratchian, H. P.; Cross, J. B.; Bakken, V.; Adamo, C.; Jaramillo, J.; Gomperts, R.; Stratmann, R. E.; Yazyev, O.; Austin, A. J.; Cammi, R.; Pomelli, C.; Ochterski, J. W.; Ayala, P. Y.; Morokuma, K.; Voth, G. A.; Salvador, P.; Dannenberg, J. J.; Zakrzewski, V. G.; Dapprich, S.; Daniels, A. D.; Strain, M. C.; Farkas, O.; Malick, D. K.; Rabuck, A. D.; Raghavachari, K.; Foresman, J. B.; Ortiz, J. V.; Cui, Q.; Baboul, A. G.; Clifford, S.; Cioslowski, J.; Stefanov, B. B.; Liu, G.; Liashenko, A.; Piskorz, P.; Komaromi, I.; Martin, R. L.; Fox, D. J.; Keith, T.; Al-Laham, M. A.; Peng, C. Y.; Nanayakkara, A.; Challacombe, M.; Gill, P. M. W.; Johnson, B.; Chen, W.; Wong, M. W.; Gonzalez, C.; Pople, J. A. *Gaussian 03*, Revision B.05; Gaussian, Inc.: Wallingford, CT, 2004; *Gaussian 03W*, Revision C.02; Gaussian, Inc.: Wallingford, CT, 2004.
- (52) Berglund, B.; Lindgren, J.; Tegenfeldt, J. *J. Mol. Struct.* **1978**, *43*, 169.
- (53) Marcus, Y. *Ion Solvation*; John Wiley & Sons, Ltd: Chichester, U.K., 1985.
- (54) Marcus, Y. *Chem. Rev.* **1988**, *88*, 1475.
- (55) Ohtaki, H.; Radnai, T. *Chem. Rev.* **1993**, *93*, 1157.